Draft version March 3, 2022
Typeset using LaTeX **twocolumn** style in AASTeX62

arXiv:1802.00493v1 [astro-ph.SR] 1 Feb 2018

2MASS J13243553+6358281 IS AN EARLY T-TYPE PLANETARY-MASS OBJECT IN THE AB DORADUS MOVING GROUP

Jonathan Gagné,[1,2] Katelyn N. Allers,[3] Christopher A. Theissen,[4] Jacqueline K. Faherty,[5] Daniella Bardalez Gagliuffi,[5] and Étienne Artigau[6]

[1] *Carnegie Institution of Washington DTM, 5241 Broad Branch Road NW, Washington, DC 20015, USA*
[2] *NASA Sagan Fellow*
[3] *Department of Physics and Astronomy, Bucknell University, Lewisburg, PA 17837, USA*
[4] *Center for Astrophysics and Space Sciences, University of California, San Diego, 9500 Gilman Dr., Mail Code 0424, La Jolla, CA 92093, USA*
[5] *Department of Astrophysics, American Museum of Natural History, Central Park West at 79th St., New York, NY 10024, USA*
[6] *Institute for Research on Exoplanets, Université de Montréal, Département de Physique, C.P. 6128 Succ. Centre-ville, Montréal, QC H3C 3J7, Canada*

(Received January 29, 2018; Revised January 31, 2018; Accepted February 1, 2018)

Submitted to ApJL

ABSTRACT

We present new radial velocity and trigonometric parallax measurements indicating that the unusually red and photometrically variable T2 dwarf 2MASS J13243553+6358281 is a member of the young ($\sim$150 Myr) AB Doradus moving group based on its space velocity. We estimate its model-dependent mass in the range 11–12 $M_{\rm Jup}$ at the age of the AB Doradus moving group, and its trigonometric parallax distance of 12.7 ± 1.5 pc makes it one of the nearest known isolated planetary-mass objects. The unusually red continuum of 2MASS J13243553+6358281 in the near-infrared was previously suspected to be caused by an unresolved L+T brown dwarf binary, although it was never observed with high-spatial resolution imaging. This new evidence of youth suggests that a low surface gravity may be sufficient to explain this peculiar feature. Using the new parallax we find that its absolute J-band magnitude is $\sim$0.4 mag fainter than equivalent-type field brown dwarfs, suggesting that the binary hypothesis is unlikely. The fundamental properties of 2MASS J13243553+6358281 follow the spectral type sequence of other known high-likelihood members of the AB Doradus moving group. The effective temperature of 2MASS J13243553+6358281 provides the first precise constraint on the L/T transition at a known young age, and indicates that it happens at a temperature of $\sim$1150 K at $\sim$150 Myr, compared to $\sim$1250 K for field brown dwarfs.

Keywords: stars: individual (2MASS J13243553+6358281) — methods: data analysis — stars: kinematics and dynamics — proper motions — brown dwarfs

1. INTRODUCTION

The recent discovery of isolated planetary-mass objects (e.g., Liu et al. 2013; Gagné et al. 2015a; Schneider et al. 2016b; Kellogg et al. 2016; Gagné et al. 2017) and widely separated planetary-mass companions (Chauvin et al. 2005; Naud et al. 2014; Gauza et al. 2015) in a range of ages provides a picture of how the atmospheres of planetary-mass objects evolve with time. The absence of a much brighter host star in their vicinity makes it possible to obtain high-resolution and high signal-to-noise spectra of their atmospheres with currently available facilities. These data are providing the foundations for our interpretation of the atmospheric features of directly imaged gas giant exoplanets such as 51 Eri b (Macintosh et al. 2015). Recent work has demonstrated overall similarities between such planetary-mass objects and giant planets at similar temperatures in their atmospheric features, but also significant differences caused mainly by their lower surface gravities. These include an excess flux in the K band caused by weakened collision-induced

jgagne@carnegiescience.edu

absorption of the H_2 molecule, compounded by a redder continuum slope at near-infrared wavelengths caused by thicker clouds (e.g., see Allers & Liu 2013; Gagné et al. 2015b; Faherty et al. 2016). Recent work has also indicated tentative evidence that there may exist a correlation between low surface gravity and the presence of high-amplitude photometric variability (Metchev et al. 2015; Naud et al. 2017; Gagné et al. 2017; Biller et al. 2017), but the small sample size still prevents a solid confirmation of this trend.

Because substellar objects cool down as they age (Burrows et al. 2001), one of the main strategies to identify planetary-mass objects has been to focus on young associations with a well-known age, which provides a way to estimate masses based on observed temperatures and evolutionary models. The nearest young associations have a few members within 10 pc of the Sun (e.g., Gagné et al. 2017), making them compelling laboratories to identify the lowest-mass objects in magnitude-limited surveys. However, their proximity means that their members are spread on large areas of the sky, making it hard to identify new members at a high confidence without measuring their full 6-dimensional kinematics. This includes the XYZ Galactic coordinates and UVW space velocity, which require measurements of the trigonometric parallax and radial velocity. Several methods were introduced to identify the most promising candidate members of young associations before measuring their radial velocity and distance (e.g., Malo et al. 2013; Gagné et al. 2014; Riedel et al. 2017; Shkolnik et al. 2017), but all of them suffer from relatively low recovery rates and high rates of contamination for the nearest associations.

A new Bayesian tool, BANYAN Σ (Gagné et al. 2018), was recently built to identify members of young associations, with an updated method and new kinematic models for the associations based on the first data release of the Gaia mission (Lindegren et al. 2016) which provided 2 million parallaxes for nearby bright stars. This tool served as the base to start the BASS-Ultracool survey (J. Gagné et al., in preparation; see also Gagné et al. 2015a, 2017; and Bardalez Gagliuffi et al. 2018), an all-sky search for isolated planetary-mass objects in 2MASS (Skrutskie et al. 2006) and AllWISE (Wright et al. 2010; Kirkpatrick et al. 2014), with a particular focus on objects in the T spectral class where clouds migrate to depths below their photosphere and methane becomes apparent in their spectra (Burgasser et al. 2006). As part of this work, the known substellar object 2MASS J13243553+6358281 (2MASS J1324+6358 hereafter) was identified as a candidate member of the 149^{+51}_{-19} Myr-old (Bell et al. 2015) AB Doradus moving group (ABDMG; Zuckerman et al. 2004), based on its sky position and proper motion only.

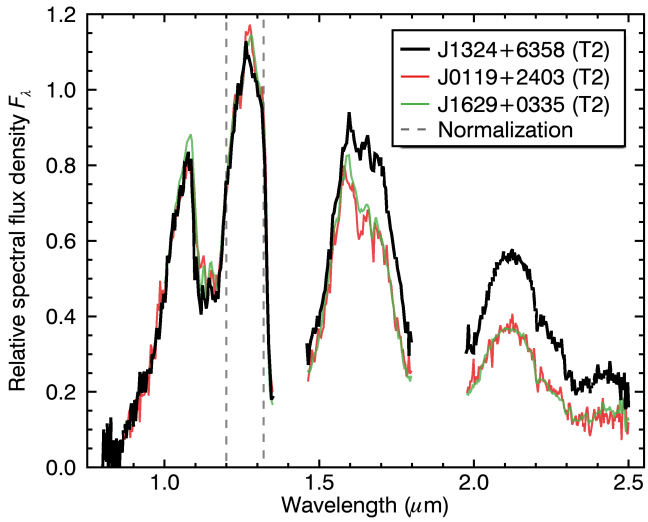


Figure 1. Relative spectral energy distribution of 2MASS J1324+6358 compared with two field T2 dwarfs. 2MASS J1324+6358 has a much redder slope, which was previously identified as a sign of either a young age or an unresolved L9 + T2 binary.

Here, we report the first measurements of a trigonometric parallax and radial velocity based respectively on data from the *WISE* survey and a new mid-resolution GNIRS spectrum, which indicate that 2MASS J1324+6358 has kinematics consistent with the locus of ABDMG members. This is a strong indication that it is a young, low-gravity T dwarf in ABDMG, and makes it unnecessary to invoke binarity to explain its peculiar spectroscopic features. We review relevant literature data on 2MASS J1324+6358 in Section 2. In Section 3, we detail the new GNIRS spectrum that was used to measure its radial velocity. The kinematics of 2MASS J1324+6358 are measured using these new data and *WISE* astrometry in Section 4, where its membership to ABDMG is also detailed. The fundamental properties of 2MASS J1324+6358 are discussed in Section 5, and this work is concluded in Section 6.

2. LITERATURE DATA

2MASS J1324+6358 was identified as a substellar object by Looper et al. (2007), and was noted for its unusually red slope in the near-infrared (see Figure 1). It was hypothesized that the most likely causes of this peculiar feature were either that this object has a very young age (estimated at <300 Myr) or that it consists of an unresolved binary with spectral types estimated at L9 + T2. Metchev et al. (2008) independently discovered this object and noted that its [4.5 μm]−[5.8 μm] IRAC

color is redder than any known T dwarf. Burgasser et al. (2010) also posited that its peculiar spectral features may be due to binarity, but they noted that it was best fit by combining a T2 dwarf with 2MASS J10430758+2225236 (Cruz et al. 2007), one of the reddest known objects classified as an optical L8 dwarf. No high-angular resolution imaging has been obtained yet for 2MASS J1324+6358.

Gagné et al. (2014) previously led an investigation of the potential young moving group membership of unusually red brown dwarfs with the BANYAN II Bayesian classifier, and only obtained a 2.4% probability that 2MASS J1324+6358 is a member of ABDMG. However, they used near-infrared color magnitude diagrams that were extrapolated at spectral types > L7 because late-type young objects were unknown at the time, and they indicated that their results should be interpreted with care at these late spectral types. These color-magnitude diagrams were responsible for missing 2MASS J1324+6358 as a candidate member of ABDMG, as ignoring them yields a 84% membership with BANYAN II using sky position and proper motion.

3. OBSERVATIONS

An intermediate-resolution near-infrared spectrum was obtained for 2MASS J1324+6358 in good weather conditions with the GNIRS spectrograph (Elias et al. 2006) at the Gemini North telescope on UT 2018 January 5. Order 3 of the 110.5 l/mm grating with a central wavelength setting of 2.3 μm was used with the 0.05″/pix long camera and the 0.″15 slit, yielding a resolving power $\lambda/\Delta\lambda$ ∼14,000 over 2.27–2.33 μm. The target was nodded along the slit in a 6″-wide ABBA pattern for 13 exposures of 600 s each, yielding a median signal-to-noise ratio per pixel of ∼ 40. Standard calibrations consisting of six 20 s flat field exposures and two 80 s Xe, Ar arc lamps were also obtained to correct pixel sensitivity and obtain an initial wavelength solution.

The data were reduced using a modified version of `REDSPEC`, Keck Observatory's facility data reduction package for high-resolution, near-infrared spectra. The reduction included an initial wavelength calibration (using sky emission lines as well as Xe, Ar arc lamps), flat-fielding and bad-pixel masking. Each nod pair was subtracted to eliminate sky emission, and the resulting A-B images were spatially and spectrally rectified. Spectra were extracted from these A-B images using an aperture equal to 0.67 times the full width at half maximum of the seeing and subtracting residual sky lines using background windows without significant source flux. Uncertainties were calculated by propagating Poisson noise throughout the reduction process. The extracted spectra were combined using a robust weighted mean with the `xcombspec` procedure from the `Spextool` package (Cushing et al. 2004).

4. KINEMATICS

4.1. *Radial Velocity*

A forward model for the GNIRS spectrum was built from radial velocity-shifted BT-Settl (CIFIST) atmosphere models (Allard et al. 2012) convolved with a rotational broadening profile, including a second-degree polynomial wavelength solution. The `atran` model for Mauna Kea (Lord 1992)[1] was then included with optical depth as a free parameter to model telluric absorption, and the resulting spectrum was convolved with a Gaussian line spread function to represent instrumental effects. The best-fitting values for these 7 forward model parameters were explored with a DREAM-ZS Markov Chain Monte Carlo method (ter Braak & Vrugt 2008), where values of $\log g$ and $T_{\rm eff}$ between grid points are explored by interpolating the nearest BT-Settl models on the grid. The corresponding Markov chains were used to build the probability density functions of the radial velocity and projected rotational velocity. A 4% systematic uncertainty was included in the data before performing this analysis so that the median uncertainties of the data match the median absolute residuals of the best fit. This resulted in a radial velocity of $-23.7^{+0.4}_{-0.2}$ km s^{-1} and a projected rotational velocity of $v \sin i = 11.5^{+1.0}_{-0.8}$ km s^{-1}. The model $\log g$ and $T_{\rm eff}$ values obtained from this forward fitting are $5.30^{+0.02}_{-0.01}$ dex and $1304.0^{+1.7}_{-1.5}$ K respectively, however such measurements for substellar objects based on fitting atmosphere models are unreliable especially when obtained from a narrow wavelength range (Gagné et al. 2015b; Filippazzo et al. 2015; Allers et al. 2016). This method is described in detail in Allers et al. (2016), where it is used to derive the radial velocity and projected rotational velocity of PSO J318.5–22 from a GNIRS spectrum obtained in the same configuration. The resulting best-fitting model is presented in Figure 2.

4.2. *Trigonometric Parallax*

The trigonometric parallax of 2MASS J1324+6358 was measured with a slight adaptation of the method described by Theissen (2017). In summary, all individual astrometric epochs of 2MASS J1324+6358 in the $W1$ and $W2$ bands were collected from all phases of the *WISE* mission[2] (providing a total baseline of 6.5 yr), and compared to a parallax and proper motion solution

[1] Calculated at a zenith angle of 48° with 3.1 mm of water vapor, see https://atran.sofia.usra.edu/cgi-bin/atran/atran.cgi

[2] *WISE* All-Sky, *WISE* 3-Band Cryo, *WISE* Post-Cryo and NEOWISE Reactivation.

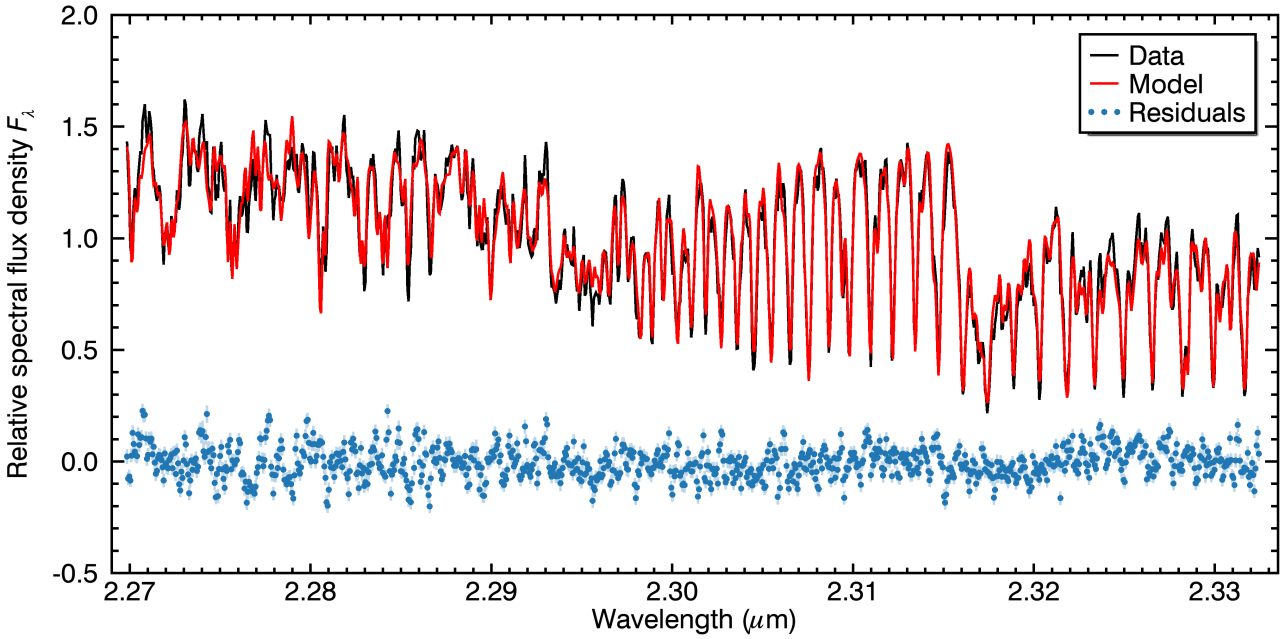


Figure 2. Best-fitting forward model (red) compared to the GNIRS spectrum of 2MASS J1324+6358 obtained here (black). Residuals are shown as blue dots. We obtain a reduced $\chi^2 = 2.3$.

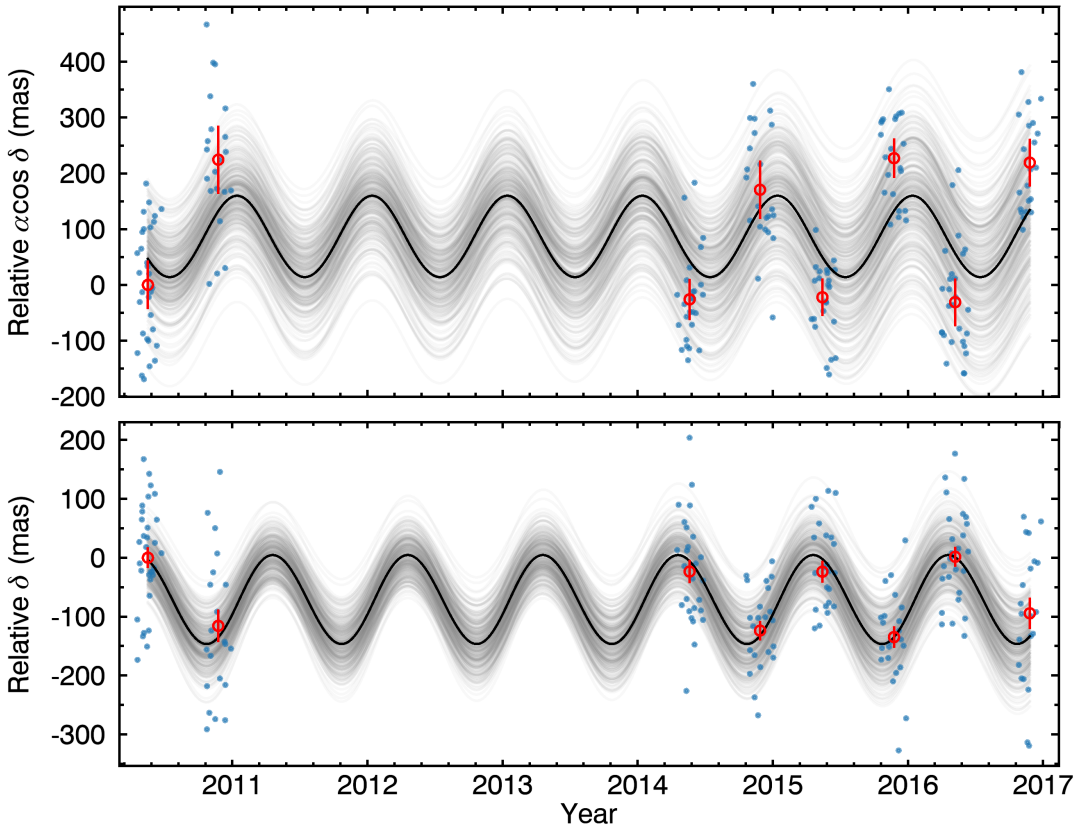


Figure 3. Relative astrometry of 2MASS J1324+6358 in right ascension and declination (red circles) with proper motion subtracted, compared to the best-fitting model (black line) and 300 random realizations selected in the Markov chains (gray lines). The blue dots are individual astrometric measurements used to build the 8 astrometric epochs with the method of Theissen (2017).

Table 1. Properties of 2MASS J13243553+6358281

Property	Value	Reference
Position and Kinematics		
R.A.	13:24:45.894 ±55 mas	1
Decl.	+63:58:12.76 ±28 mas	1
Epoch (JD)	2455334.4 ±0.5[a]	1
$\mu_\alpha \cos\delta$ (mas yr^{-1})	-379.7 ± 7.7	2
μ_δ (mas yr^{-1})	-66.2 ± 7.0	2
Radial velocity (km s^{-1})	$-23.7^{+0.4}_{-0.2}$	1
Parallax (mas)	78.7 ± 9.0	1
Trigonometric distance (pc)	12.7 ± 1.5	1
X (pc)	-3.5 ± 0.4	1
Y (pc)	6.9 ± 0.8	1
Z (pc)	10.1 ± 1.2	1
U (km s^{-1})	-9.5 ± 1.9	1
V (km s^{-1})	-28.8 ± 1.9	1
W (km s^{-1})	-13.6 ± 0.7	1
Photometric Properties		
$i_{\rm AB}$ (SDSS)	22.73 ± 0.28	3
$z_{\rm AB}$ (SDSS)	18.72 ± 0.04	3
J (2MASS)	15.60 ± 0.07	4
H (2MASS)	14.58 ± 0.06	4
K (2MASS)	14.06 ± 0.06	4
$W1$ (AllWISE)	13.12 ± 0.02	5
$W2$ (AllWISE)	12.29 ± 0.02	5
$W3$ (AllWISE)	10.78 ± 0.07	5
[3.6 μm] (IRAC)	12.56 ± 0.03	6
[4.5 μm] (IRAC)	12.33 ± 0.03	6
[5.8 μm] (IRAC)	11.79 ± 0.03	6
[8.0 μm] (IRAC)	11.31 ± 0.03	6
Fundamental Properties		
Spectral type	T2 ±1	6,7
Age (Myr)	149^{+51}_{-19}	1,8
Mass ($M_{\rm Jup}$)	11–12	1
Radius ($R_{\rm Jup}$)	1.23 ± 0.02	1
$T_{\rm eff}$ (K)	1080 ± 60	1
$\log g$	4.29 ± 0.02	1
$\log L_*/L_\odot$	-4.72 ± 0.10	1
Rotation period (h)	13 ± 1	9
$v \sin i$ (km s^{-1})	$11.5^{+1.0}_{-0.8}$	1
i (°)	56^{+11}_{-7}	1

[a]This corresponds to the first combined epoch in the WISE measurements, where the error bar is given by the standard deviation of the individual epochs that were combined.

References—(1) This work, (2) Schneider et al. 2016a, (3) Alam et al. 2015, (4) Skrutskie et al. 2006, (5) Kirkpatrick et al. 2014, (6) Metchev et al. 2008, (7) Looper et al. 2007, (8) Bell et al. 2015, (9) Metchev et al. 2015

with the Markov Chain Monte Carlo Python package `emcee` (Foreman-Mackey et al. 2013). The method of Theissen (2017) has only 3 free parameters corresponding to the parallax and the two dimensions of proper motion, and compares the forward parallax model to all 8 astrometric epochs relative to the first measurement. To avoid propagating the information of the first measurement across all epochs, we included the average sky position of 2MASS J1324+6358 as two additional free parameters. This modification makes this analysis less vulnerable to outlier measurements, and yields more conservative error bars on all parameters. The resulting parallax measurement is 78.7 ± 9.0 mas, with a proper motion of $\mu_\alpha \cos\delta = -378.3 \pm 10.4$ mas yr^{-1} and $\mu_\delta = -68.0 \pm 5.7$ mas yr^{-1}. The best-fitting astrometric solution is displayed in Figure 3. As explained by Theissen (2017), this astrometric solution does not include a correction for the motion of background stars. They estimated a parallax correction of the order of 2 mas, well within the error bar for the parallax, but not for the proper motion, and we therefore adopt the proper motion measurement of Schneider et al. (2016a; based on 2MASS and AllWISE with a 10.4 yr baseline), which is reported in Table 1 with our parallax measurement.

4.3. *Kinematic Membership to Nearby Young Associations*

The BANYAN Σ algorithm was used to determine the Bayesian probability that 2MASS J1324+6358 is a member of young associations within 150 pc of the Sun. The sky position, proper motion, radial velocity and trigonometric parallax distance of 2MASS J1324+6358 (see Table 1) were used and yielded an ABDMG membership probability of 98.0%. The measured UVW space velocity of 2MASS J1324+6358 (see Table 1) is located within 1.1 km s^{-1} of the locus of ABDMG members compiled in Gagné et al. (2018), within the velocity dispersion of the moving group (1.4 km s^{-1}), corresponding to a 0.7σ distance in the kinematics tri-dimensional space when accounting for the covariances in the distribution of existing ABDMG members. The Galactic coordinates XYZ of 2MASS J1324+6358 are located at ∼22.7 pc from the core of ABDMG members, corresponding to a 1.1 σ distance from the core of the BANYAN Σ model. ABDMG has a relatively large characteristic size of ∼19 pc in XYZ space (Gagné et al. 2018).

5. FUNDAMENTAL PROPERTIES

5.1. *Color-Magnitude Diagram*

The trigonometric parallax measured in Section 4.2 allows us to place 2MASS J1324+6358 in a color-magnitude diagram and compare it with the sequence of field brown

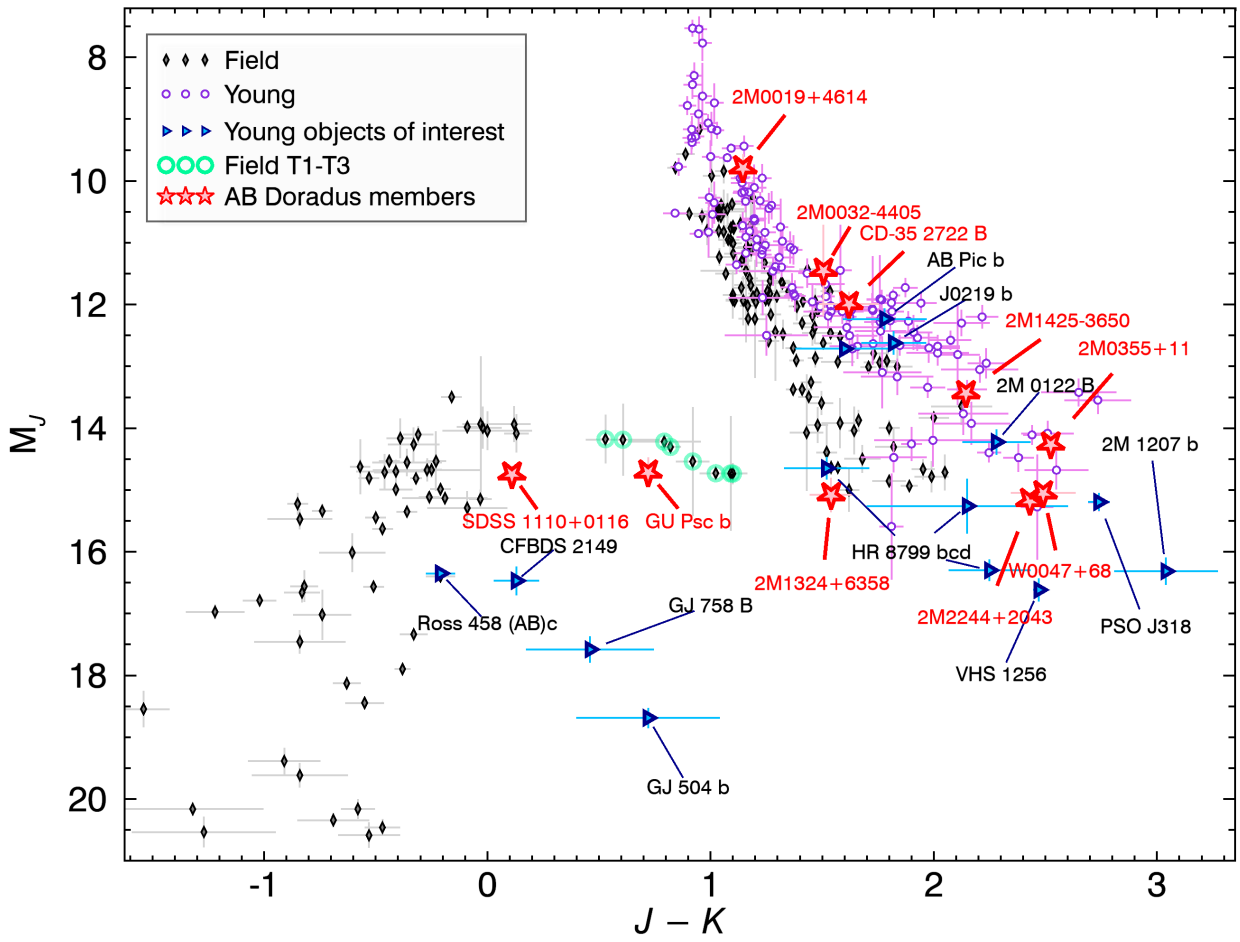


Figure 4. Color-magnitude diagram of confirmed or high-likelihood members of ABDMG (as defined by Faherty et al. 2016) with trigonometric parallax measurements (red stars) compared with field (black diamonds) and young brown dwarfs (open purple circles and right-pointing blue triangles). Field brown dwarfs within one spectral subtype of 2MASS J1324+6358 are marked with a green open circle. The ABDMG members define a sequence redder than the field, with an L/T transition happening at a slightly fainter J-band magnitude. 2MASS J1324+6358 is both redder and fainter than field T1–T3 dwarfs in the near-infrared, similarly to young late-type L dwarfs. These data were compiled from Gagné et al. (2015b), Faherty et al. (2016), Liu et al. (2016), Vos et al. (2018) and other references therein.

dwarfs (Figure 4). 2MASS J1324+6358 falls in sequence with other young members of ABDMG, redder in $J - K$ than field brown dwarfs, and where the L/T transition takes place at a slightly fainter J-band magnitude. This L/T transition magnitude dependence on age was hinted by the properties of the HR 8799 bcd planets (Marois et al. 2008; Marley et al. 2012) and those of the ABDMG members SDSSp J111010.01+011613.1 and GU Psc b (Gagné et al. 2015a; Naud et al. 2014; see also the discussion of Liu et al. 2016), but 2MASS J1324+6358 provides yet stronger evidence for this effect.

5.2. *Multiplicity*

The fainter J-band magnitude of 2MASS J1324+6358 compared to the field substellar sequence goes against the spectral binary hypothesis, unless there is a large J-band contrast ratio between the two components, which would be inconsistent with the best-fitting L9 + T2 components identified by Looper et al. (2007) and Burgasser et al. (2010). If we assume that 2MASS J1324+6358 is an equal-mass binary with a conservative mass estimate in the range 5–60 $M_{\rm Jup}$ based on L9 + T2 spectral types at any age, our inability to resolve doubled spectral lines with the GNIRS spectrum corresponds to a weak lower limit in physical separation in the range 0.02–0.22 AU, or an angular separation of $\sim$1.6–17.3 mas at the measured trigonometric parallax distance. The absence of elongation in the point-spread function of the GNIRS acquisi-

tion images[3] puts an upper limit on the separation of an equal-luminosity binary at $\sim 0\farcs2$, or ~ 2.5 AU. The fact that the kinematics of 2MASS J1324+6358 are consistent with a membership in ABDMG is sufficient to explain its peculiar spectroscopic features, as described in Section 2. As a consequence of these considerations, we consider the binary hypothesis as highly unlikely. This is also consistent with the general picture that high variability in substellar objects seems to be correlated with low surface gravity and thus youth (Metchev et al. 2015; Gagné et al. 2017). The case of 2MASS J1324+6358 would also be reminiscent of 2MASS J21392676+0220226, which was first identified as a candidate L8.5 + T4.5 spectral binary by Burgasser et al. (2010). Radigan et al. (2012) later ruled out the presence of a companion at separations above ~ 1.6 AU for a J-band constrast of 3 mag or less using *HST*/NICMOS imaging, and discovered it to be highly variable with a 26% peak-to-peak J-band amplitude. This suggested that the high variability of brown dwarfs may be due to evolving and rotating patterns of patchy clouds, presenting us a combination of more than a single atmospheric layer at different effective temperatures. We can therefore suspect that highly variable brown dwarfs will cause more false positives in the detection of binaries with the spectral fitting method.

5.3. *Spectral Energy Distribution*

The trigonometric parallax measured here was combined with the 0.8–2.5 μm low-resolution near-infrared spectrum of Looper et al. (2007) and all photometric data listed in Table 1 (i.e. SDSS, 2MASS, AllWISE and IRAC) to build the spectral energy distribution of 2MASS J1324+6358. The method described in Filippazzo et al. (2015) and Faherty et al. (2016) was then used to directly measure its bolometric luminosity, estimate a radius and a mass based on the Saumon & Marley (2008) evolutionary models at the age of ABDMG, and translate the radius and bolometric luminosity to a semi-empirical effective temperature using the Stefan-Boltzmann law. The resulting fundamental properties of 2MASS J1324+6358 are listed in Table 1. 2MASS J1324+6358 falls in sequence with other high-likelihood ABDMG members (see Figure 4) in spectral type, mass, temperature and $\log L_*/L_\odot$ measured with the same method (Gagné et al. 2015a; Faherty et al. 2016), although its mass estimate overlaps significantly with that of the L6–L8 γ-type bona fide member 2MASS J22443167+2043433 (Vos et al. 2018). The temperatures of 2MASS J22443167+2043433 (1180 ± 10 K; Faherty et al. 2016) and 2MASS J1324+6358 (1080 ± 60 K) provide an indication that the transition from the L to T spectral type happens at ~ 1150 K at the age of ABDMG, a temperature slightly cooler than for field-aged brown dwarfs (~ 1250 K; Filippazzo et al. 2015). This is consistent with previous observations in the literature (e.g., see Metchev & Hillenbrand 2006; Liu et al. 2016).

5.4. *Geometric Radius Constraint*

The rotation period of 2MASS J1324+6358 was measured from its *Spitzer*/IRAC light curves in the [3.5 μm] and [4.3 μm] bands by Metchev et al. (2015), who found an approximate period of 13 ± 1 h. The probability distribution for the inclination of 2MASS J1324+6358 was explored with a Markov Chain Monte Carlo analysis based on geometry with the radius estimate and the projected rotational velocity reported in Table 1. A non-informative prior probability on the inclination $P(i) = \sin i$ was adopted. We obtain an estimate of $i = 56^{+11}_{-7}{}^\circ$. Measurements of both the photometric period and projected rotational velocity also make it possible to derive a lower limit on the radius of 2MASS J1324+6358 which ensures $v \sin i \leq v$, in a model-independent way. A 10^7-elements Monte Carlo approach was performed to account for the measurement errors and yielded a lower limit of $1.22 \pm 0.2\,R_{\rm Jup}$ on its radius, independent of evolutionary models. Comparing this limit with the Saumon & Marley (2008) models at the measured bolometric luminosity provides an upper limit of 150^{+150}_{-130} Myr on the age of 2MASS J1324+6358, independent of kinematics and consistent with membership in ABDMG.

6. CONCLUSIONS

A new trigonometric parallax based on the *WISE* mission astrometry and a radial velocity measured from a GNIRS near-infrared spectrum are presented for 2MASS J1324+6358 and suggest that it is a member of the young ~ 150 Myr-old ABDMG. This fact alone could explain the spectroscopic peculiarities first noted by Looper et al. (2007) without the need to invoke an unresolved L9 + T2 spectral binary. The trigonometric parallax places 2MASS J1324+6358 in line with the sequence of other ABDMG members, at a much redder $J-K$ color than field T1-T3 dwarfs and a slightly fainter J-band magnitude, providing more evidence that the L/T transition at a young age happens at a fainter magnitude in this particular color-magnitude space, and at a cooler effective temperature.

We thank the anonymous referee of this letter for a prompt and useful report. We thank Matthew Taylor,

[3] Available at the Gemini Science Archive at https://archive.gemini.edu

Sandy Leggett, Tom Geballe, and Lucas Fuhrman for their help with the GNIRS observing, and Jack Gallimore for his contributions to the DREAM-ZS fitting code. This research made use of: data products from the Two Micron All Sky Survey (2MASS), which is a joint project of the University of Massachusetts and the Infrared Processing and Analysis Center (IPAC)/California Institute of Technology (Caltech), funded by the National Aeronautics and Space Administration (NASA) and the National Science Foundation; data products from the *Wide-field Infrared Survey Explorer* (*WISE*), which is a joint project of the University of California, Los Angeles, and the Jet Propulsion Laboratory (JPL)/Caltech, funded by NASA. Based on observations obtained at the Gemini Observatory (science program number GN-2017B-FT-21) acquired through the Gemini Observatory Archive, which is operated by the Association of Universities for Research in Astronomy, Inc., under a cooperative agreement with the NSF on behalf of the Gemini partnership: the National Science Foundation (United States), the National Research Council (Canada), CONICYT (Chile), Ministerio de Ciencia, Tecnología e Innovación Productiva (Argentina), and Ministério da Ciência, Tecnologia e Inovação (Brazil).

Software: BANYAN Σ (Gagné et al. 2018), BANYAN II (Gagné et al. 2014), emcee (Foreman-Mackey et al. 2013).

Facilities: Gemini: North (GNIRS).

REFERENCES

Alam, S., Albareti, F. D., Allende Prieto, C., et al. 2015, The Astrophysical Journal Supplement Series, 219, 12

Allard, F., Homeier, D., & Freytag, B. 2012, Philosophical Transactions of the Royal Society A: Mathematical, 370, 2765

Allers, K. N., Gallimore, J. F., Liu, M. C., & Dupuy, T. J. 2016, The Astrophysical Journal, 819, 133

Allers, K. N., & Liu, M. C. 2013, The Astrophysical Journal, 772, 79

Bardalez Gagliuffi, D. C., Gagné, J., Faherty, J. K., & Burgasser, A. J. 2018, arXiv.org, 1801.06134v1

Bell, C. P. M., Mamajek, E. E., & Naylor, T. 2015, Monthly Notices of the Royal Astronomical Society, 454, 593

Biller, B., Vos, J., Buenzli, E., et al. 2017, arXiv.org, arXiv:1712.03746

Burgasser, A. J., Cruz, K. K., Cushing, M. C., et al. 2010, The Astrophysical Journal, 710, 1142

Burgasser, A. J., Geballe, T. R., Leggett, S. K., Kirkpatrick, D. J., & Golimowski, D. A. 2006, The Astrophysical Journal, 637, 1067

Burrows, A., Hubbard, W. B., Lunine, J. I., & Liebert, J. 2001, Reviews of modern physics, 73, 719

Chauvin, G., Lowrance, P., Lagrange, A.-M., et al. 2005, Astronomy and Astrophysics, 438, L25

Cruz, K. L., Reid, I. N., Kirkpatrick, J. D., et al. 2007, The Astronomical Journal, 133, 439

Cushing, M. C., Vacca, W. D., & Rayner, J. T. 2004, The Publications of the Astronomical Society of the Pacific, 116, 362

Elias, J. H., Joyce, R. R., Liang, M., et al. 2006, Ground-based and Airborne Instrumentation for Astronomy. Edited by McLean, 6269, 62694C

Faherty, J. K., Riedel, A. R., Cruz, K. L., et al. 2016, The Astrophysical Journal Supplement Series, 225, 10

Filippazzo, J. C., Rice, E. L., Faherty, J., et al. 2015, The Astrophysical Journal, 810, 158

Foreman-Mackey, D., Conley, A., Meierjurgen Farr, W., et al. 2013, Astrophysics Source Code Library, ascl:1303.002

Gagné, J., Burgasser, A. J., Faherty, J. K., et al. 2015a, The Astrophysical Journal Letters, 808, L20

Gagné, J., Lafrenière, D., Doyon, R., Malo, L., & Artigau, É. 2014, The Astrophysical Journal, 783, 121

Gagné, J., Faherty, J. K., Cruz, K. L., et al. 2015b, The Astrophysical Journal Supplement Series, 219, 33

Gagné, J., Faherty, J. K., Burgasser, A. J., et al. 2017, The Astrophysical Journal Letters, 841, L1

Gagné, J., Mamajek, E. E., Malo, L., et al. 2018, arXiv.org, arXiv:1801.09051

Gauza, B., Béjar, V. J. S., Pérez-Garrido, A., et al. 2015, The Astrophysical Journal, 804, 96

Kellogg, K., Metchev, S., Gagné, J., & Faherty, J. 2016, The Astrophysical Journal Letters, 821, L15

Kirkpatrick, D. J., Schneider, A. C., Fajardo-Acosta, S., et al. 2014, The Astrophysical Journal, 783, 122

Lindegren, L., Lammers, U., Bastian, U., et al. 2016, Astronomy & Astrophysics, 595, A4

Liu, M. C., Dupuy, T. J., & Allers, K. N. 2016, The Astrophysical Journal, 833, 96

Liu, M. C., Magnier, E. A., Deacon, N. R., et al. 2013, The Astrophysical Journal Letters, 777, L20

Looper, D. L., Kirkpatrick, J. D., & Burgasser, A. J. 2007, The Astronomical Journal, 134, 1162

Lord, S. D. 1992, NASA Technical Memorandum 103957

Macintosh, B., Graham, J. R., Barman, T., et al. 2015, Science, 350, 64

Malo, L., Doyon, R., Lafrenière, D., et al. 2013, The Astrophysical Journal, 762, 88

Marley, M. S., Saumon, D., Cushing, M., et al. 2012, The Astrophysical Journal, 754, 135

Marois, C., Macintosh, B., Barman, T. S., et al. 2008, Science, 322, 1348

Metchev, S. A., & Hillenbrand, L. A. 2006, The Astrophysical Journal, 651, 1166

Metchev, S. A., Kirkpatrick, D. J., Berriman, G. B., & Looper, D. 2008, The Astrophysical Journal, 676, 1281

Metchev, S. A., Heinze, A., Apai, D., et al. 2015, The Astrophysical Journal, 799, 154

Naud, M.-E., Artigau, É., Rowe, J. F., et al. 2017, The Astronomical Journal, 154, 138

Naud, M.-È., Artigau, É., Malo, L., et al. 2014, The Astrophysical Journal, 787, 5

Radigan, J., Jayawardhana, R., Lafrenière, D., et al. 2012, The Astrophysical Journal, 750, 105

Riedel, A. R., Blunt, S. C., Lambrides, E. L., et al. 2017, The Astronomical Journal, 153, 95

Saumon, D., & Marley, M. S. 2008, The Astrophysical Journal, 689, 1327

Schneider, A. C., Greco, J., Cushing, M. C., et al. 2016a, The Astrophysical Journal, 817, 112

Schneider, A. C., Windsor, J., Cushing, M. C., Kirkpatrick, J. D., & Wright, E. L. 2016b, The Astrophysical Journal Letters, 822, L1

Shkolnik, E. L., Allers, K. N., Kraus, A. L., Liu, M. C., & Flagg, L. 2017, The Astronomical Journal, 154, 69

Skrutskie, M. F., Cutri, R. M., Stiening, R., et al. 2006, The Astronomical Journal, 131, 1163

ter Braak, C. J. F., & Vrugt, J. A. 2008, Statistics and Computing, 18, 435

Theissen, C. A. 2017, arXiv.org, arXiv:1710.11127

Vos, J. M., Allers, K. N., Biller, B. A., et al. 2018, Monthly Notices of the Royal Astronomical Society, 474, 1041

Wright, E. L., Eisenhardt, P. R. M., Mainzer, A. K., et al. 2010, The Astronomical Journal, 140, 1868

Zuckerman, B., Song, I., & Bessell, M. S. 2004, The Astrophysical Journal, 613, L65